

Infrared Constrains on AGN Tori Models

Evanthia Hatziminaoglou (1), the SWIRE Team

(1) *Instituto de Astrofísica de Canarias, C/ Vía Láctea s/n, 38300 La Laguna, Spain*

Abstract. This work focuses on the properties of dusty tori in active galactic nuclei (AGN) derived from the comparison of SDSS type 1 quasars with mid-Infrared (MIR) counterparts and a new, detailed torus model. The infrared data were taken by the Spitzer Wide-area InfraRed Extragalactic (SWIRE) Survey. Basic model parameters are constraint, such as the density law of the graphite and silicate grains, the torus size and its opening angle. A whole variety of optical depths is supported. The favoured models are those with decreasing density with distance from the centre, while there is no clear tendency as to the covering factor, i.e. small, medium and large covering factors are almost equally distributed. Based on the models that better describe the observed SEDs, properties such as the accretion luminosity, the mass of dust, the inner to outer radius ratio and the hydrogen column density are computed. The properties of the tori, as derived fitting the observed SEDs, are independent of the redshift, once observational biases are taken into account.

1. Torus Model

A detailed description of the torus model is given in Fritz et al. (2006); here we briefly present the main characteristics. The adopted torus geometry is a *flared disk*, i.e. a sphere with the polar cones removed. Its size is defined by its outer radius, R_{out} , and its opening angle. The dust components that dominate both the absorption and the emission of radiation are graphite and silicate. The inner radius, R_{in} , depends both on the sublimation temperature of the dust grains (1500 and 1000 K, for graphite and silicate, respectively) and on the accretion luminosity. Since silicate grains have a lower sublimation temperature than graphite grains, the innermost regions of the torus only consist of graphite. The adopted absorption and scattering coefficients are those by Laor & Drain (1993) for dust grains of different dimensions, weighted with the standard MRN distribution (Mathis et al. 1977). The gas density within the torus is modeled in such a way to allow a gradient along both the radial and the angular coordinates.

The central source is assumed to be point-like and its emission isotropic. Its spectral energy distribution is defined by means of a composition of power laws with different values for the spectra index in the UV, optical and IR. The Λ -iteration method is used to solve the radiative transfer equation. A geometrical grid is defined along the three spatial coordinates, and the main physical quantities (dust density and temperatures, electromagnetic emission, optical depth, etc.) are computed with respect to the center of the volume elements defined by the grid. The global SED is computed at different angles of the line-of-sight with

respect to the torus' equatorial plane and includes three contributions: emission from the AGN, thermal emission and scattering emission by dust in each volume element. An example of an emitted spectrum is given in Fig. 1.

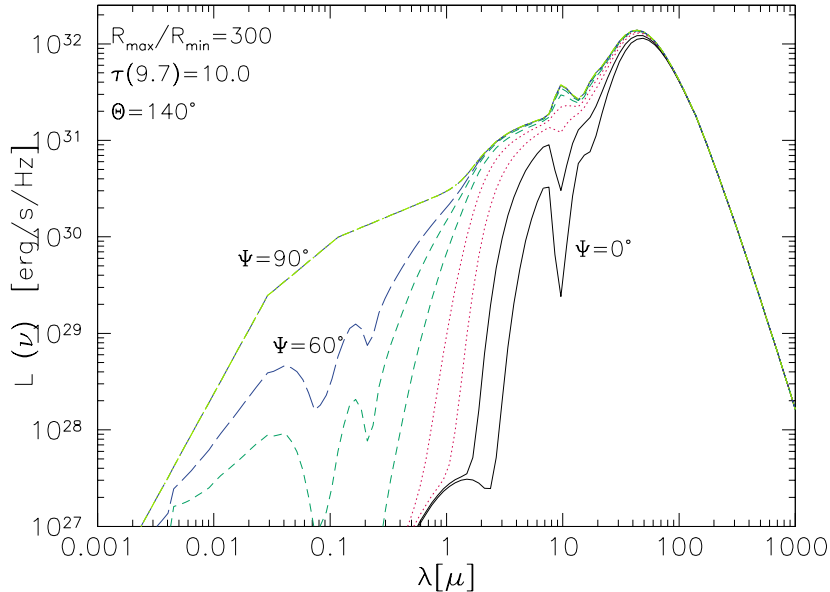


Figure 1. Emission spectra as a function of wavelength for 10 different lines-of-sight inclinations from $\Psi = 0^\circ$ (edge-on; lower curve) to $\Psi = 90^\circ$ (face-on, upper curve) at regular steps of 10° , for a geometrical configuration with $\tau(9.7) = 10.0$, $R_{\text{out}}/R_{\text{in}} = 300$, torus opening angle $\Theta = 140^\circ$ and density law $\rho(r, \theta) \propto r^{-1} e^{-6|\cos(\theta)|}$, where r is the distance from the centre and θ the angle from the equatorial plane.

2. Data

The MIR data used here are taken from the SWIRE EN1 and EN2 and Lockman fields and the SWIRE catalogues processed by the SWIRE collaboration. Details about the data can be found in Lonsdale et al. (2004), Surace et al. (2005) and Shupe et al. (2006). The optical data were taken from the Sloan Digital Sky Survey (SDSS) Data Release 4 (DR4), that covers the entire Lockman and SWIRE EN2 fields and a part of the SWIRE EN1 field. 2MASS data points were also used, whenever available as well as data from the Deep 2MASS Survey in Lockman (Beichman et al. 2003).

A total of 279 spectroscopically confirmed quasars, all detected in all IRAC bands and MIPS 24 micron, lie within the SWIRE fields covered by the SDSS DR4 spectroscopic release, with redshifts spanning from 0.214 to 5.215. Their i -band magnitudes reach 19.1 for objects with redshifts typically less than 2.3 and go up to a magnitude deeper for higher redshifts (Richards et al. 2002). For a detailed analysis of the properties of the sample in EN1 see Hatziminaoglou et al. (2005).

3. First Results and Implications

Each observed SED is compared to a total of 720 models, with 10 lines of sight each (from an equatorial to a pole-on view). Examples of best fits are shown in Fig. 2. Some of the results of the SED fitting are summarised below.

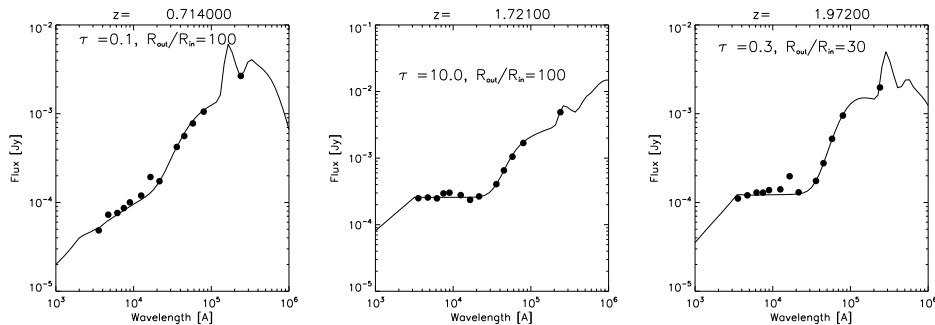


Figure 2. Examples of SED fits for three AGN of our sample. The fluxes are given in Jy, the wavelengths in Å.

For $\sim 70\%$ of the objects the density, $\rho(r, \theta) \propto r^\beta e^{-\gamma|\cos(\theta)|}$, decreases radially from the centre ($\beta < 0$) while for another $\sim 25\%$ it remains constant ($\beta = 0$). Half of the objects have a density distribution that does not vary with the angle, θ , from the equator. Trying not to exclude *a priori* any of the model characteristics, we allow for low optical depth tori. Some 65% of the objects were better described by models with $\tau_{9.7} < 1.0$. We therefore need to recalculate the covering factor and consider that we switch from a type 1 to a type 2 object (i.e. that we no longer see the central source through the torus) when $\tau_{0.3} > 1$.

Inner radii are typically of order of a few pc, with extreme cases (very luminous objects) reaching ~ 10 pc, as seen on the left panel of Fig. 3. The mass of dust, M_{Dust} , is computed summing the individual sample elements of the best-fit model. Typical values range from 10^4 to $10^6 M_\odot$. Note that M_{Dust} does not refer to the total mass of the torus, that can be obtained by adding the mass of gas, typically ~ 100 times larger than that of the dust. Many quantities (R_{in} , R_{out} , M_{Dust} ,...) show a clearly increasing trend with redshift, z . This could be interpreted as an indication for larger and/or more massive tori at higher z ; however it is simply the manifestation of the Scott effect, i.e. the fact that in order for distant objects to make it into a flux-limited sample they need to be intrinsically brighter. What happens in reality is that the inner radius, R_{in} , directly scales with the accretion luminosity, L_{acc} (expressed in units of 10^{46} erg/sec), via the relation by Barvainis (1987): $R_{\text{in}} \simeq 1.3 \times \sqrt{L_{\text{acc}}} \times T_{1500}^{-2.8}$ [pc], where the temperature, T , is given in units of 1500K. In a flux-limited sample L_{acc} , which is directly related to the bolometric luminosity, increases with z and therefore so does R_{in} , as well as R_{out} and M_{Dust} that directly depend on R_{in} , as already mentioned. We therefore deduce that sources of the same accretion luminosity can have similar properties, independently on the redshift.

The *equatorial* hydrogen column density, N_{H} , distribution, derived from the models, is shown in the right panel of Fig. 3. The values are representative of type 2 objects, with some in the range of Compton thick AGN ($N_{\text{H}} \sim 10^{24}$

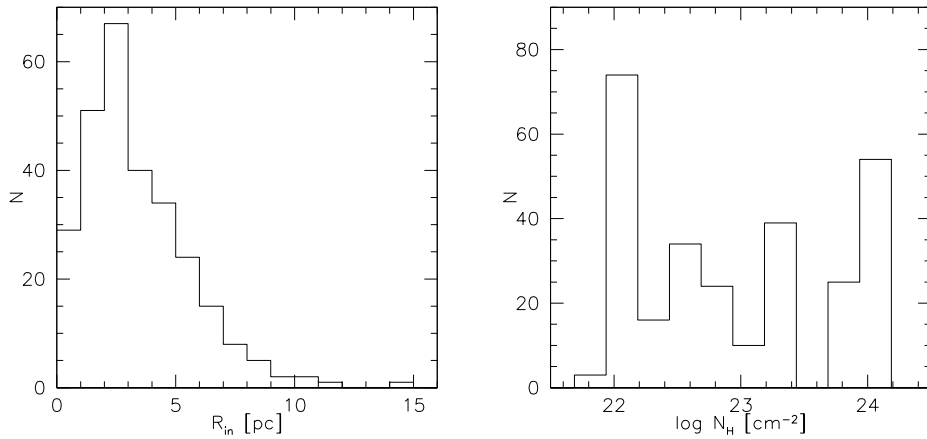


Figure 3. Left panel: histogram of the inner torus radii, R_{in} ; Right panel: distribution of the hydrogen column density, N_H , along the equator.

cm^{-2}). If the distinction between type 1 and type 2 objects is simply a matter of orientation, as suggested from the Unified Scheme, this would be the expected distribution of *equatorial* N_H .

4. Conclusions

This work in progress provides useful insights into the properties of dusty tori around AGN. Fitting the observed optical-to-MIR SEDs to a series of models, we showed that in most of the cases the density decreases with distance from the centre and can vary with the angle from the equator. Tori properties such as the outer radii or the mass of dust are independent of the redshift and only depend on the luminosity of the objects. The *equatorial* hydrogen column density distribution is in agreement with what is expected from the Unified Scheme.

Acknowledgments. This work is based on observations made with the *Spitzer Space Telescope*. It also makes use of the SDSS and 2MASS Archives. It was supported in part by the Spanish Ministerio de Educación y Ciencia (Grant Nr. ESP2004-06870-C02-01).

References

- Barvainis R., 1987, ApJ, 320, 537
- Beichman C.A. et al., 2003, AJ, 125, 2521
- Fritz J., Franceschini A. & Hatziminaoglou E., 2006, MNRAS, 366, 767
- Hatziminaoglou E. et al., 2005, AJ, 129, 1198
- Laor A. & Drain B.T., 1993, ApJ, 402, 441
- Lonsdale C. et al., 2004, ApJS, 154, 54
- Mathis J.S., Rumpl W. & Nordsieck K.H., 1977, ApJ, 217, 425
- Richards G.T. et al., 2002, AJ, 123, 2945
- Shupe D.L. et al., 2006, AJ, submitted
- Surace J. et al., 2005, SWIRE Data Release Document